Processing and Application of Ceramics 18 [2] (2024) 196–202
https://doi.org/10.2298/PAC2402196A

Synthesis of TiB_2 powders by borothermal and carbothermal reduction of TiO_2

Mohamed Mahrous Hussein Abdelgawad[1], Hülya Biçer[1,2,*]

[1]*Department of Metallurgy and Materials Engineering, Kütahya Dumlupınar University, 43000, Kütahya, Turkey*
[2]*Boron Based Advanced Ceramics Application and Research Center (BORSAM), Kütahya Dumlupınar University, 43000, Kütahya, Turkey*

Received 18 March 2024; Received in revised form 29 May 2024; Accepted 17 June 2024

Abstract

Titanium diboride powders were synthesized from TiO_2 following different reduction methods at temperatures range from 1000 to 1400 °C for 1 h under flowing argon gas. The reduction processes used in this study are classified as TiO_2 + B (borothermal reduction), TiO_2 + H_3BO_3 + C (carbothermal reduction) and TiO_2 + B + C (combined reduction). XRD peaks of TiO_2 phase are present for each sample below 1100 °C. It was also observed that XRD peaks of TiO_2 disappeared and TiB_2 was formed in borothermal and combined reduction methods at temperature of 1100 °C and above. In the carbothermal method, $TiBO_3$ and TiC phases were present at these temperatures and TiB_2 could only be obtained after heat treatment at 1400 °C. However, this temperature also caused considerable particle growth and formation of the powders with hexagonal shape morphology. The powders synthesized by the carbon-containing reduction process contained residual carbon.

Keywords: *borides, TiB_2, solid state synthesized powders, carbothermal borothermal reduction*

I. Introduction

Transition metal borides (ZrB_2, TiB_2, HfB_2, etc.) are actively used in various applications due to their superior properties and promising applications in many fields. Transition metal borides (TMBs) have high melting points. Their excellent thermal stability, oxidation resistance and high hardness make these materials suitable for extreme environments. Moreover, TMBs have low electrical resistance and high thermal conductivity. Such materials have been extensively studied and investigated as bulk materials [1–3]. Metal borides with an AlB_2 type structure have attracted attention for new research areas due to the natural presence of boron atoms arranged in a honeycomb pattern reminiscent of graphenic arrangement. Therefore, interest in fabrication of these borides at nanoscale is also increasing [4]. In recent years, various non-noble catalysts have been reported that have the potential to replace current electrodes used in water electrolysers, and among these, metal boride powders stand out with their balance of price and performance [5,6]. Moreover, very recently, electrochemical performances of metal boride powders as electrodes for all-in-one symmetric and asymmetric supercapacitor devices have been investigated [7,8]. From this broader family of materials, TiB_2 exhibits high hardness (25–35 GPa), high melting point (3000 °C), good thermal conductivity (~65 $Wm^{-1}K^{-1}$), high electrical conductivity and remarkable chemical stability [9]. In addition to the potential use of TiB_2 powder in electrochemical applications mentioned above, there are some other application areas of TiB_2. The physical and mechanical properties of ceramic and metal matrix composites are improved by utilizing TiB_2 powder as an additive for grain refinement and particle strengthening [10,11]. TiB_2 is used as a crucible for non-ferrous metals and as a cathode for the electrolysis of molten alumina in a Hall-Heroult cell due to its resistance to molten metals, high electrical conductivity and corrosion resistance at high temperatures [12]. TiB_2 is also utilized in defence industry applications owing to its relatively low density, high fracture toughness and good hardness [13].

* Corresponding author: tel: +90 274 265 2023/4325
e-mail: *hulya.bicer@dpu.edu.tr*

One of the most critical steps in ceramic production is to obtain a powder with the desired properties, including purity, morphology and particle size. A wide variety of synthesis methods are used to produce TiB_2 powders. These methods can be classified according to the phase state of the starting materials (solid, liquid or gas synthesis processes), the form of the precursors (oxides or elemental, etc.) or the types of reductants (carbon, boron, metal, etc.). Mainly, TiB_2 powders are synthesized by mechanochemical method [14], self-propagating high-temperature synthesis (SHS) [15], molten salt-assisted synthesis [16] and reduction of oxides via solid-state synthesis [17–21]. There are several advantages to employing carbothermal reductions by solid state synthesis in the production of high-tech ceramic powders, such as: use of low-cost raw materials, relatively low energy requirement and highly scalable operation, making it suitable for commercial use. TiO_2 is used as a titanium source in reduction synthesis within the solid-state method and it mainly reacts with carbon or boron. Also B_4C is used as reducing agent in some studies to obtain TiB_2 powder [17–21].

To find alternative ways of synthesizing fine, pure TiB_2 powders in a single study, carbothermal, borothermal and combined (boro/carbothermal) reduction methods were studied simultaneously using TiO_2 powder. Possible thermodynamic reactions, phase analysis and electron microscope images are reported.

II. Experimental

TiO_2 (Nanokar, 1 μm with purity of 99%), amorphous boron (Nanokar, 1 μm, 95%), H_3BO_3 (ETİ MADEN) and carbon black (Sigma Aldrich) powders were used as starting materials. The powders were weighed according to the stoichiometry summarized in Table 1 and placed in a stainless steel jar with a silicon nitride ball inside a glove box in a vacuum environment. The milling jar was sealed and transferred to the planetary mill. Each powder mixture was milled for 8 h (300 rpm) and left to cool to room temperature slowly. All powders were placed in a graphite crucible, heated with a 5 °C/min heating rate and held at the target temperature for 1 h under a 0.3 l/min argon flow. Powders were heat treated between 1000–1400 °C based on thermodynamical calculations.

Table 2 shows the reactions in TiB_2 synthesis based on the method used in this study. Most of the works synthesizing diborides by boro/carbothermal reduction mechanism reported the utilization of boron carbide. This study conducted the boro/carbothermal reduction process with boron and carbon powders as a reducing agent for TiO_2. Figure 1 exhibits the standard state of Gibbs' free energy reactions as a function of temperature made from HSC Chemistry for the synthesis routes of TiB_2 which are classified in Table 2.

The phase analysis of powders after milling and after heat treatments were examined with X-ray diffrac-

Table 1. Sample compositions and synthesis parameters

Sample designation	Raw materials (molar ratio) TiO_2	B	H_3BO_3	C	Temperature [°C]	Note
TB	3	10	-	-	1000 1100 1200	Excess boron
TBC	1	2	-	2	1000 1100 1200 1300	Excess boron
THBC	1	-	2	5	1000 1100 1200 1300 1400 1300 + 1400	Excess boric acid

Table 2. Reduction reactions for each technique

Mechanism	Reaction	Temperature	Ref.
Borothermal reduction	$3\,TiO_2 + 10\,B \longrightarrow 3\,TiB_2 + 2\,B_2O_3(g)$	Over 800 °C (under vacuum) (at 1100 °C TiB_2 major phase)	[17,18]
Boro/carbothermal reduction	$TiO_2 + 2\,B + 2\,C \longrightarrow TiB_2 + 2\,CO(g)$	1000–1100 °C	
Carbothermal reduction	$TiO_2 + 2\,H_3BO_3 + 5\,C \longrightarrow TiB_2 + 5\,CO(g) + 3\,H_2O(g)$	1000–1100 °C	

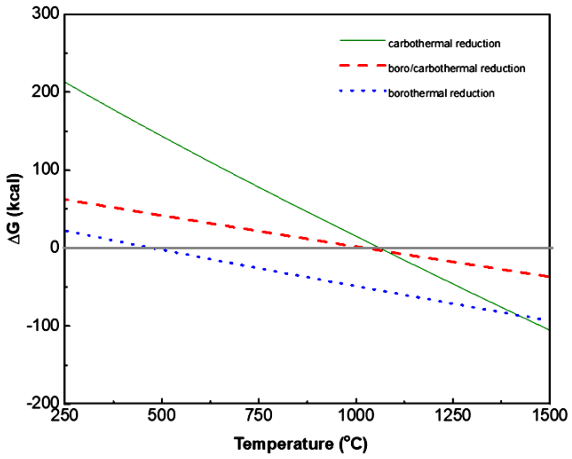

Figure 1. The standard state of Gibbs' free energy reactions as a function of temperature for the formation routes of TiB_2

tometry (Rigaku-Miniflex, using CuKα radiation, λ = 1.54178 Å), and the morphology of powders was examined with scanning electron microscopy (Nova, NanoSEM™).

III. Results and discussion

XRD analysis results of the thermally processed TB, TBC and THBC samples as a function of synthesis temperature are shown in Figs. 2, 3 and 4, respectively. Based on thermodynamic data, the formation of TiB_2 is expected to begin at temperature between 1000 and 1100 °C. The borothermal reaction in Table 2 occurs at very low temperatures based on thermodynamic predictions. However, literature studies show that the formation of the TiB_2 phase via borothermal reduction begins around 1100 °C under an inert atmosphere and as early as 800 °C under a vacuum [17,18]. The used 8-hour milling of the starting powder was insufficient to initiate intermediate reactions between the compounds for all samples without heat treatment. Moradi *et al.* [22] studied the effect of the milling time on the synthesis of TiB_2 via carbothermal reduction and confirmed that no new phase was observed by milling up to 48 h. However, it was suggested that by increasing the grinding time, the removal of undesirable phases such as C and TiC from the structure was improved [22].

XRD peaks of TiO_2 phase are present for each sample at the holding temperatures below 1100 °C, but the disappearance of the TiO_2 peaks is confirmed for the TB and TBC samples when the powders were heat-treated at temperatures of 1100 °C and above. On the other hand, contrary to the TB and TBC powders, the structure of the THBC powder heat-treated at 1100 °C is dominated by the $TiBO_3$ phase and also contains the TiC phase, formed according to following reactions:

$$2\,TiO_2 + B_2O_3 + C \longrightarrow 2\,TiBO_3 + CO(g) \quad (1)$$

$$TiO_2(s) + 3\,C \longrightarrow TiC(s) + 2\,CO(g) \quad (2)$$

These intermediate phases were also observed in a study

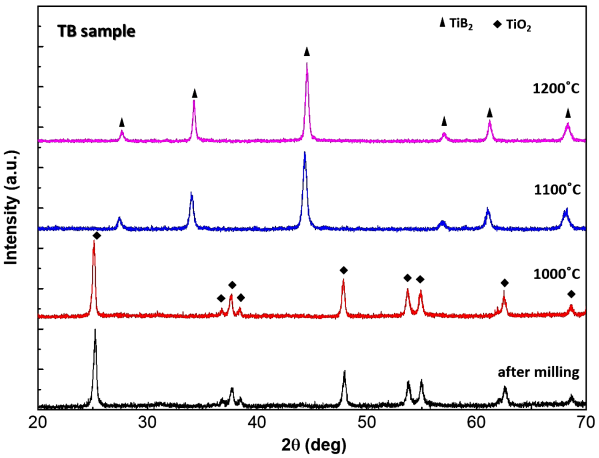

Figure 2. X-ray diffraction pattern of TB samples synthesized at different temperatures

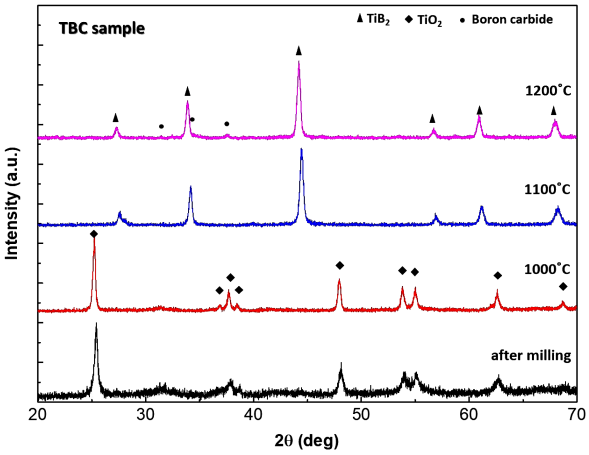

Figure 3. X-ray diffraction pattern of TBC samples synthesized at different temperatures

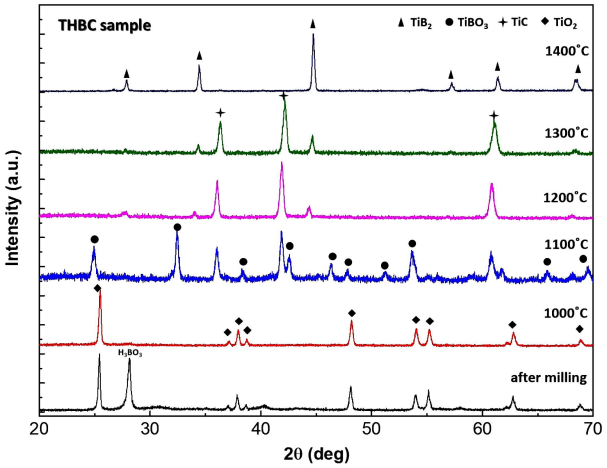

Figure 4. X-ray diffraction pattern of THBC samples synthesized at different temperatures

performed with the use of boron carbide for the production of TiB_2 powder [23]. XRD pattern of the THBC powder synthesized at 1000 °C (Fig. 4) did not reveal XRD peaks of $TiBO_3$ or Ti_nO_{2n-1} phase. The reduction of the TiO_2 phase by carbon started over 1000 °C and the formation of $TiBO_3$ by boro/carbothermal reduction followed by reaction 1 was confirmed by XRD results [24]. *Li et al.* [25] predicted the formation reaction of Ti_nO_{2n-1} (n = 3 and 5) phases between 1048 and 1152 °C. No presence of Ti_nO_{2n-1} was detected in the THBC powder synthesized between 1000 and 1200 °C in this study. Therefore reaction 1 was suggested as the reduction reaction of TiO_2. The formation of $TiBO_3$ by borothermal reduction of TiO_2 was also reported by Millet *et al.* [26] as an intermediate reaction. The XRD patterns of the TB sample, heat treated in a temperature range of 1000–1200 °C with the 100 °C interval, did not exhibit $TiBO_3$ intermediate phase since TiO_2 was reduced by boron to $TiBO_3$ and Ti_2O_3 phases below 1000 °C via borothermal reduction.

The predicted reaction 2 for the formation of TiC phase, based on HSC Chemistry software analysis, occurs at temperatures between 1285–1290 °C. As seen in Fig. 4, evidence of the formation of the TiC phase in the presence of carbon and boron without the formation of TiB_2 appeared at 1100 °C. Moreover, XRD peaks of TiC phase dominated in the structure of the THBC powder at temperatures up to 1400 °C once all $TiBO_3$ peaks disappeared. On the contrary, in the TBC powder, which was synthesized in the presence of carbon and boron, there is no evidence of TiC phase in the XRD pattern at the same temperatures. In a study where TiO_2, B_4C and carbon were used as raw materials, the TiC phase was observed alongside the TiB_2 phase up to 1450 °C and the full conversion (TiB_2 formation) was completed at 1600 °C. Kinetic factors and the reaction pathway presumably cause such observation. The XRD pattern of TBC phase (Fig. 3) demonstrates the initiation of the formation of boron carbide around 1200 °C with the use of two reduction agents, boron and carbon.

Figure 5 displays the SEM images of powders. For morphology comparison, those subjected to heat treatment at 1200 °C were selected for TB and TBC powders, and the one subjected to heat treatment at 1400 °C, where the TiB_2 phase was observed, was chosen for THBC powder. The morphology of TB and TBC particles are identical. On the other hand, TB powder consists of larger particles than TBC powder synthesized at 1200 °C (Fig. 5). The particle size of THBC is larger than other powders, and the reason for the growth of particles is the increase of synthesis temperature, which is inevitable for the formation of TiB_2 phase. To examine the effect of temperature, the SEM images of TBC powder heat-treated at 1100 and 1300 °C (the image of TBC-1200 is in Fig. 5) was demonstrated in Fig. 6. The increase in temperature yielded larger particle size and more hexagonal plate-like morphology. Higher temperature increases the crystallinity of TiB_2 phase while causing particle growth. TB and TBC powders contained magnesium impurity, resulting from commercial boron, whereas TBC and THBC powders contained residual carbon (EDS spectrum of TBC-1300 powder is shown in Fig. 6).

The THBC powder synthesized at 1300 °C was heat-treated once again at 1400 °C for 1 h and the sample is designated as THBC-1300/1400. Figure 7 shows the morphology, EDS analysis and XRD pattern of the THBC 1300/1400 powder, as well as the SEM image of the THBC-1400 powder. The dominant TiC phase seen in the structure of THBC-1300 powder totally disappeared and the TiB_2 phase formed (with the presence of free carbon) as shown in the XRD pattern of the THBC-

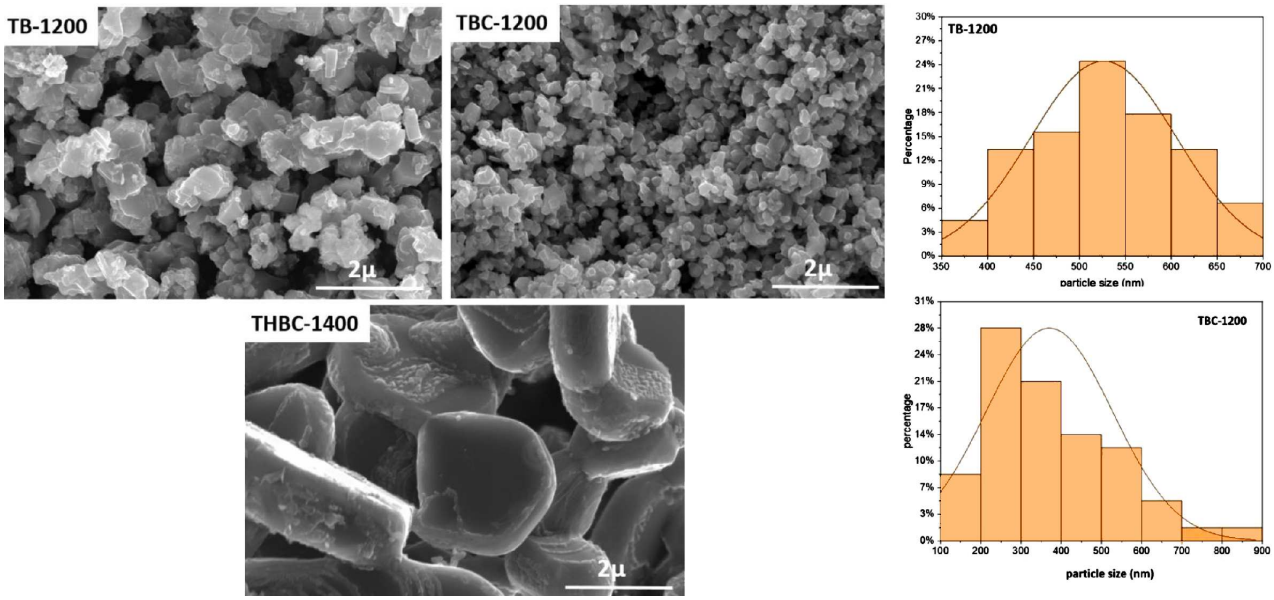

Figure 5. Morphology of TB and TBC powders synthesized at 1200 °C and THBC powder synthesized at 1400 °C, and the particle size distribution of TB and TBC powders synthesized at 1200 °C

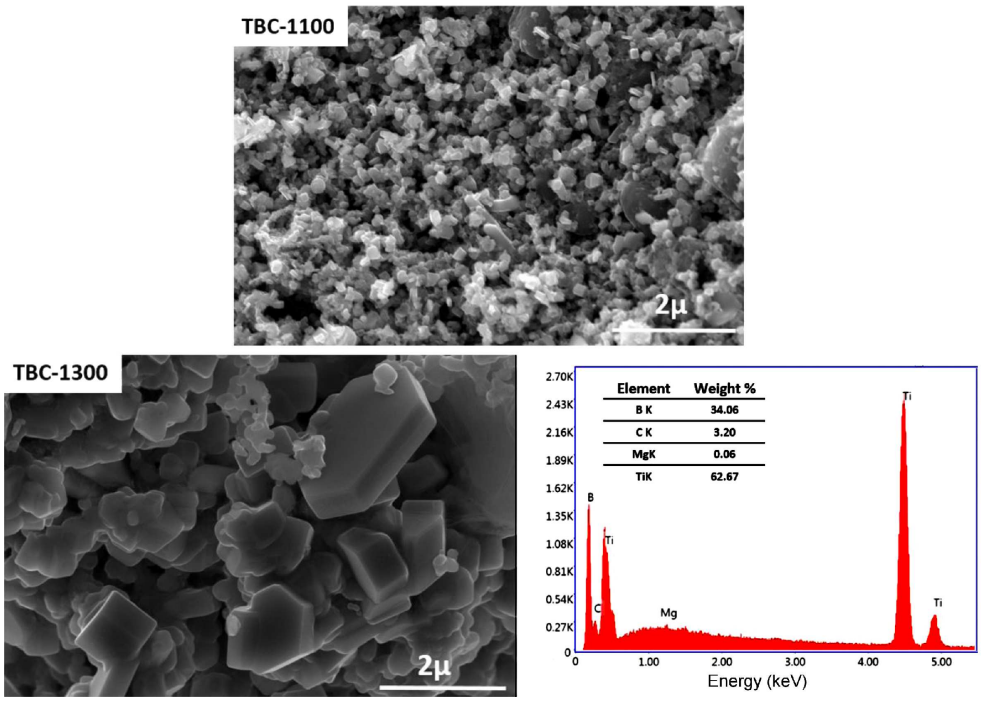

Figure 6. SEM images of TBC powder heat-treated at 1100 and 1300 °C (EDS spectra of TBC-1300 powder is also added)

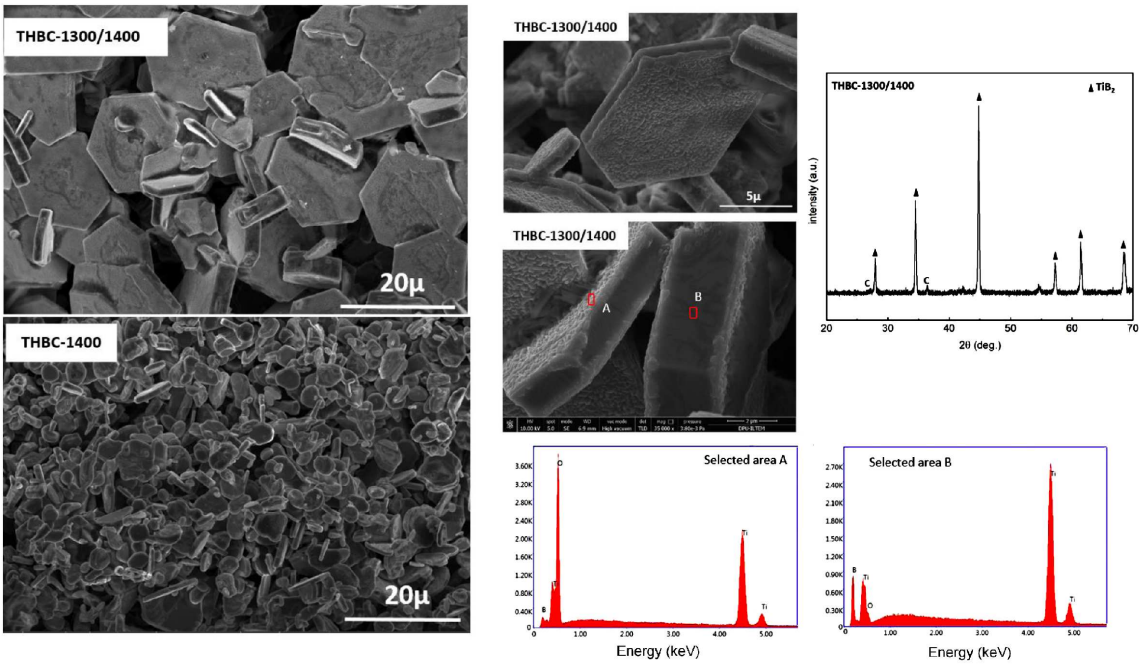

Figure 7. SEM images, EDS spectra and XRD pattern of THBC-1300/1400 sample (SEM image of THBC-1400 is also added)

1300/1400. A favourable reaction route for the formation of TiB_2 from TiC is through reaction 3:

$$TiC + 2\,C + B_2O_3 \longrightarrow TiB_2 + 3\,CO(g) \qquad (3)$$

The THBC 1300/1400 powder exhibits a particle size larger than 10 μm, which is higher than the particle size of the THBC-1400 powder. The morphology of the hexagonal type constitutes the majority of the structure of the THBC-1300/1400 powder. However, the oxidation of the particle surface is evident in the THBC-1300/1400 powder (Fig. 7). As it can also be seen from the EDS spectra and SEM micrographs in Fig. 7, at the surface of the hexagonal particles an oxide layer was formed, while the side faces contained very low amount of oxygen as a result of the oxidation kinetics dependence on the surface area. On the contrary, such oxidation behaviour is not observaed in the THBC-1400 powder (contains low oxygen level). It has been reported that the residual oxygen in TiB_2 partitions between titanium and boron to form their respective oxides, namely TiO_2 and B_2O_3 [27]. Since XRD pattern displays peaks

of only TiB_2 and carbon phases in Fig. 7, oxide layers in the structure could be in amorphous state.

IV. Conclusions

Titanium diboride powders were synthesized from TiO_2 by reduction processes (TiO_2 + B - borothermal reduction, TiO_2 + H_3BO_3 + C - carbothermal reduction and TiO_2 + B + C - combined reduction) at temperatures ranging from 1000 to 1400 °C for 1 h under flowing argon gas. Although thermodynamic calculations indicated the synthesis of TiB_2 by the borothermal reduction method at low temperatures, in practice, XRD analysis did not support the formation of TiB_2 under 1100 °C. These results are also compatible with the literature studies. The particle size of the TB powder increased with increasing temperature and is larger than that of the TBC powders synthesized at identical temperatures.

In the combined technique where both boron and carbon are used to reduce TiO_2, TiB_2 formation was not observed below 1100 °C. The hexagonal morphology structure became evident as the temperature increased, while the particle size also increased. This behaviour is also similar to the TB powder. The resulting powder contained residual carbon.

In the carbothermal reduction method, TiB_2 formation is expected in the range of 1000–1100 °C in line with thermodynamic calculations. However, due to intermediate reactions, $TiBO_3$ and TiC phases dominated the structure at 1100 and 1200 °C, respectively. The transition from TiC phase to TiB_2 phase occurred at temperatures of 1350–1400 °C. TiB_2 phase was observed as a result of heat treatment at 1400 °C in this study, and this temperature caused the considerable growth of particles. The THBC powder was also heat treated in two stages, first at 1300 °C and then at 1400 °C for 1 h. This powder is highly oxidized. The reason for this may be that after the first synthesis, the powder (in TiC form) underwent a second heat treatment with an oxide layer on the particle surfaces. Although there is oxygen contamination in the THBC sample synthesized in a single step at 1400 °C, it is very low (below 1% by weight).

Acknowledgements: This study was financially supported by The Scientific and Technological Research Council of Türkiye (TUBITAK-BIDEB) 2209-A program (period of 2022/1).

References

1. Y. Orooji, E. Ghasali, M. Moradi, M.R. Derakhshandeh, M. Alizadeh, M.S. Asl, T. Ebadzadeh, "Preparation of mullite-TiB_2-CNTs hybrid composite through spark plasma sintering", *Ceram. Int.*, **45** [13] (2019) 16288–16296.
2. S.-Q. Guo, T. Nishimura, Y. Kagawa, J.-M. Yang, "Spark plasma sintering of zirconium diborides", *J. Am. Ceram. Soc.,* **91** [9] (2008) 2848–2855.
3. Z.H. Zhang, X.B. Shen, F.C. Wang, S.K. Lee, L. Wang, "Densification behavior and mechanical properties of the spark plasma sintered monolithic TiB_2 ceramics", *Mater. Sci. Eng. A*, **527** [21-22] (2010) 5947–5951.
4. S. Chakrabarty, A. Thakur, A. Rasyotra, B. Gaykwad, K. Jasuja, "Quasi-two-dimensional nanostructures from AlB_2-type metal borides: physicochemical insights and emerging trends", *J. Phys. Chem. C*, **127** [2] (2022) 852–870.
5. S. Gupta, M.K. Patel, A. Miotello, N. Patel, "Metal boride-based catalysts for electrochemical water-splitting: A review", *Adv. Funct. Mater.,* **30** [1] (2020) 1906481.
6. Y. Kang, Y. Tang, L. Zhu, B. Jiang, X. Xu, O. Guselnikova, H. Li, T. Asahi**,** Y. Yamauchi, "Porous nanoarchitectures of nonprecious metal borides: from controlled synthesis to heterogeneous catalyst applications", *ACS Catalysis*, **12** [23] (2022) 14773–14793.
7. A. Paksoy, M. Buldu-Akturk, S. Arabi, E. Erdem, Ö. Balcı-Çağıran, "Synthesis and capacitive performance of ZrB_2 and its composites as supercapacitor electrodes", *Solid State Sci*., **142** (2023) 107256.
8. M. Buldu-Akturk, B.-Ç. Özge, E. Erdem, "EPR investigation of point defects in HfB_2 and their roles in supercapacitor device performances", *Appl. Phys. Lett.,* **120** [15] (2022) 153901.
9. B. Basu, G.B. Raju, A.K. Suri. "Processing and properties of monolithic TiB_2 based materials", *Int. Mater. Rev.,* **51** [6] (2006) 352–374.
10. S. Suresh, N. Shenbag, V. Moorthi, "Aluminium-titanium diboride (Al-TiB_2) metal matrix composites: challenges and opportunities", *Procedia Eng.*, **38** (2012) 89–97.
11. X. Yue, S. Zhao, P. Lü, Q. Chang, H. Ru, "Synthesis and properties of hot pressed B_4C-TiB_2 ceramic composite", *Mater. Sci. Eng. A*, **527** [27-28] (2010) 7215–7219.
12. I.A. Blokhina, V.V. Ivanov, S.D. Kirik, N.S. Nikolaeva, "Carbothermal synthesis of TiB_2 powders of micron size", *Inorg. Mater*., **52** (2016) 550–557.
13. Ö. Kaya, "Silisyum Karbür Ve Grafen Nano Plaka (gnp) Takviyeli Titanyum Diborür Seramiklerin Spark Plazma Sinterleme Yöntemi İle Üretimi Ve Karakterizasyonu", Diss. Fen Bilimleri Enstitüsü, 2016
14. W.M. Tang, Z.X. Zheng, Y.C. Wu, J.M. Wang, J. Lü, J.W. Liu Jun-wu, "Synthesis of TiB_2 nanocrystalline powder by mechanical alloying", *Tran. Nonferrous Metals Soc. China*, **16** [3] (2006) 613–617.
15. N. Chaichana, N. Meemongkol, J. Wannasin, S. Niyomwas,"Synthesis of nano-sized TiB_2 powder by self-propagating high temperature synthesis", *CMU J. Nat. Sci.*, **7** [1] (2008) 51–57.
16. F. Akkurt, K. Emine, Y. Abdulkerim, "Üstün özelliklere sahip ileri teknoloji seramiği: Titanyum diborür", *J. Boron*, **4** [4] (2019) 203–208.
17. W.M. Guo, G.-J. Zhang, Y. You, S.-H. Wu, H.-T. Lin, "TiB_2 powders synthesis by borothermal reduction in TiO_2 under vacuum", *J. Am. Ceram. Soc.*, **97** [5] (2014) 1359–1362.
18. Z. Fu, R. Koc, "Synthesis of TiB_2 from a carbon-coated precursors method", *J. Am. Ceram. Soc.*, **100** [6] (2017) 2471–2481.
19. S.H. Kang, D.J. Kim, "Synthesis of nano-titanium diboride powders by carbothermal reduction", *J. Eur. Ceram. Soc.*, **27** [2-3] (2007) 715–718.
20. S.E. Bates, W.E. Buhro, C.A. Frey, Shankar, M.L. Sastry, K.F. Kelton , "Synthesis of titanium boride (TiB_2)

nanocrystallites by solution-phase processing", *J. Mater. Res.*, **10** [10] (1995) 2599–2612.
21. R.L. Axelbaum, D.P. DuFaux, C.A. Frey, K.F. Kelton, S.A. Lawton, L.J. Rosen, S.M.L. Sastry, "Gas-phase combustion synthesis of titanium boride (TiB_2) nanocrystallites", *J. Mater. Res.*, **11** [4] (1996) 948–954.
22. V. Moradi, L. Nikzad, I. Mobasherpour, M. Razavi, "Low temperature synthesis of titanium diboride by carbothermal method", *Ceram. Int.*, **44** [16] (2018) 19421–19426.
23. L-Y. Zeng, W.-X. Wei, S.-K. Sun, W.-M. Guo, H. Li, H.-T. Lin, "Powder characteristics, sinterability, and mechanical properties of TiB_2 prepared by three reduction methods", *J. Am. Ceram. Soc.*, **102** [8] (2019) 4511–4519.
24. N.J. Welham, "Mechanical enhancement of the carbothermic formation of TiB_2", *Metal. Mater. Trans. A*, **31** (2000) 283–289.
25. X. Li, X. Wang, J. Tang, B. Chen, J. Qiao, "Low-temperature synthesis of high-purity TiB_2 via carbothermal reduction of metatitanic acid and H_3BO_3", *Ceram. Int.*, **49** [24] (2023) 40140–40148.
26. P. Millet, T. Hwang, "Preparation of TiB_2 and ZrB_2. Influence of a mechano-chemical treatment on the borothermic reduction of titania and zirconia", *J. Mater. Sci.*, **31** (1996) 351–355.
27. T.E. Özdemir, E.K. Akdoğan, İ. Şavklıyıldız, H. Biçer, M. Örnek, Z. Zhong, T. Tsakalakos, "Electric field effect on chemical and phase equilibria in nano-TiB_2-TiO_2-$TiBO_3$ system at < 650 °C: An in situ time-resolved energy dispersive x-ray diffraction study with an ultrahigh energy synchrotron probe", *J. Mater. Res.*, **32** [2] (2017) 482–494.